Note: Three wavelengths near-infrared spectroscopy system for compensating the light absorbance by water

M. Raheel Bhutta,[1] Keum-Shik Hong,[1,2,a)] Beop-Min Kim,[3] Melissa Jiyoun Hong,[4] Yun-Hee Kim,[5] and Se-Ho Lee[1]
[1]*Department of Cogno-Mechatronics Engineering, Pusan National University, Busan 609–735, South Korea*
[2]*School of Mechanical Engineering, Pusan National University, Busan 609–735, South Korea*
[3]*Department of Biomedical Engineering, Korea University, Seoul 136–703, South Korea*
[4]*Department of Education Policy and Social Analysis, Columbia University, New York, New York 10027, USA*
[5]*Department of Physical and Rehabilitation Medicine, Sungkyunkwan University School of Medicine, Seoul 135–710, South Korea*

(Received 25 September 2013; accepted 27 January 2014; published online 12 February 2014)

Given that approximately 80% of blood is water, we develop a wireless functional near-infrared spectroscopy system that detects not only the concentration changes of oxy- and deoxy-hemoglobin (HbO and HbR) during mental activity but also that of water (H_2O). Additionally, it implements a water-absorption correction algorithm that improves the HbO and HbR signal strengths during an arithmetic task. The system comprises a microcontroller, an optical probe, tri-wavelength light emitting diodes, photodiodes, a WiFi communication module, and a battery. System functionality was tested by means of arithmetic-task experiments performed by healthy male subjects. © *2014 AIP Publishing LLC*. [http://dx.doi.org/10.1063/1.4865124]

Near-infrared spectroscopy (NIRS), first introduced by Jobsis,[1] is a noninvasive method that monitors physiological changes such as blood volume and tissue oxygenation by using the optical properties of the tissue in the spectral window of 600–1000 nm. In this window of light, the main absorbers of light are the blood chromophores, oxy-hemoglobin (HbO), and deoxy-hemoglobin (HbR), and water (H_2O). The absorption by lipids and the other chromophores therein are relatively smaller, though these chromophores can yet affect the absorbance of light. A complete knowledge of NIRS techniques and its associated methods is already provided in the previous literature.[2–6] A variety of NIRS-based systems have been utilized in fields such as neuroscience,[7–9] neuropsychology,[10] and brain computer interface.[11,12] However, most of these systems are not easily portable and do not enable complete freedom of motion, which limits their research applications. A few researches with more than two wavelengths have already been published[13,14] and the effect of water on other chromophores is already been discussed,[15] but in most of the studies the concentration change of HbO and HbR is analyzed and no one has implemented a dynamic water correction algorithm to enhance the strengths of HbO and HbR. More recently, Muehlemann *et al.*[16] designed a small portable four-channel NIRS system. The contributions of the present study are: (i) a completely developed 12-channel wireless NIRS system that incorporates three wavelength light emitters for measurement of HbO, HbR, and H_2O concentration changes, and (ii) a dynamic algorithm that corrects the absorbed light by water for the improvement of HbO and HbR signal strengths during mental activity.

The hardware of the developed wireless NIRS system consists of two major components: a data acquisition module and a data processing module. The data acquisition module controls the light emission to the subject body and detection of scattered light using photodiodes. It then transmits the collected data wirelessly to the data processing module. The data acquisition module has two main components: (i) an optical probe on which light emitters and detectors are strategically arranged; and (ii) control and operation electronics consisting of a microcontroller, drive circuitry, a WiFi module, and a power supply. The optical probe is a flexible PCB and consists of three tri-wavelength light-emitting diodes (LEDs) (SMT 640/700/910, Epitex, Japan) and eight photodiodes (FDS1010 – Si Photodiode, ThorLabs, USA). Each LED can emit three wavelengths (640, 700, and 910 nm) lights at 3 mW/sr, 10 mW/sr, and 18 mW/sr radiant intensity, respectively. Each photodiode, having a photo sensitivity of 0.3 A/W at 640 nm, 0.4 A/W at 700 nm, and 0.58 at 910 nm, can detect light of 400–1100 nm wavelength range with an active area of 9.7 × 9.7 mm. Each emitter and neighboring detector pair constitutes one channel. Since each emitter has four neighboring detectors, the system includes a total of 12 channels. The source to detector distance is about 3 cm. The photodiodes are synchronized with the LEDs such that the emitted light is detected only by neighboring photodiodes. The control and operation electronics consist of a microcontroller (dsPIC33FJ256MC710A, Microchip Technologies, USA), drive circuitry, a WiFi module, and a power supply. The transimpedance circuit converts a photodiode's light-intensity signal to voltage. This analog voltage value is then digitized by the microcontroller's 12-bit analog to digital converter. The microcontroller also controls the switching between different wavelengths of three LEDs and the activation of the respective neighboring photodiodes. A total of 36 data values are collected in one sample (3 emitters × 3 wavelengths × 4 neighboring detectors). The sampling rate of the system is about 40 Hz. The digitized light-intensity data are

a)Author to whom correspondence should be addressed. Electronic mail: kshong@pusan.ac.kr.

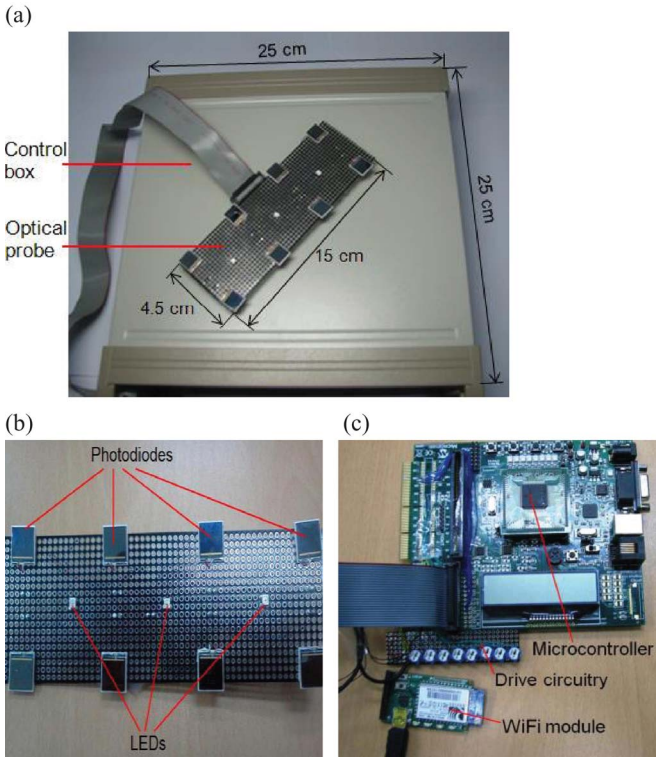

FIG. 1. Wireless LED-based NIRS system: (a) complete NIRS system, (b) optical probe, (c) control and operation electronics.

serially transmitted to an 802.11 b/g WiFi module (RN131 EK, Roving Network, USA), which subsequently transmits them wirelessly to the data processing module. The design of the power-supply circuitry demands a special attention, as different voltages are needed for the microcontroller (3.3 V), and LEDs and photodiodes (5 V each). A lithium-polymer battery (LiPo 12000XL 2-cell 7.4v, Maxamps, USA) powers the NIRS system. The voltage is down-regulated to fulfill the system requirements. Fig. 1 shows the complete NIRS system with its size and detailed internal circuitry of each block. As already noted, the digitized light-intensity data are transmitted, wirelessly by WiFi, to the data processing module. Therein, a C#-based graphical user interface (GUI) receives the data from the WiFi channel and stores it in a text file that can be used online or in real time. HbO, HbR, and H_2O concentration changes are calculated at each time instant by using the modified Beer-Lambert law (MBLL):[17]

$$\begin{bmatrix} \Delta c_{\mathrm{HbO}} \\ \Delta c_{\mathrm{HbR}} \\ \Delta c_{\mathrm{H_2O}} \end{bmatrix} = \begin{bmatrix} l d^{\lambda_1} \alpha_{\mathrm{HbO}}^{\lambda_1} & l d^{\lambda_1} \alpha_{\mathrm{HbR}}^{\lambda_1} & l d^{\lambda_1} \alpha_{\mathrm{H_2O}}^{\lambda_1} \\ l d^{\lambda_2} \alpha_{\mathrm{HbO}}^{\lambda_2} & l d^{\lambda_2} \alpha_{\mathrm{HbR}}^{\lambda_2} & l d^{\lambda_2} \alpha_{\mathrm{H_2O}}^{\lambda_2} \\ l d^{\lambda_3} \alpha_{\mathrm{HbO}}^{\lambda_3} & l d^{\lambda_3} \alpha_{\mathrm{HbR}}^{\lambda_3} & l d^{\lambda_3} \alpha_{\mathrm{H_2O}}^{\lambda_3} \end{bmatrix}^{-1} \times \begin{bmatrix} \Delta A_1 \\ \Delta A_2 \\ \Delta A_3 \end{bmatrix}, \quad (1)$$

where Δc_{HbO}, Δc_{HbR}, and Δc_{H2O} are the concentration changes of oxy-hemoglobin, deoxy-hemoglobin, and water, d is the differential pathlength factor (DPF) which is wavelength dependent, l is the distance between the emitter and the detector, the α weights, which are wavelength dependent, are the absorption coefficients of the respective chromophores, λ_1, λ_2, and λ_3 are the three wavelengths of emitters (in this study λ_1 is 640 nm, λ_2 is 700 nm, and λ_3 is 910 nm), ΔA_1, ΔA_2, and ΔA_3 are the change of absorbance depending upon λ_1, λ_2, and λ_3, respectively. The DPF values in Zhao *et al.*[18] were used in the reconstruction of hemodynamic signals. The absorption coefficients were taken from UCL website.[20] Once the concentration changes of HbO, HbR, and H_2O are determined, we can find the exact value of absorption change for all three wavelengths by using Eq. (2):

$$\Delta\mu_{\mathrm{a}}(k, \lambda_i) = \alpha_{\mathrm{HbO}}(\lambda_i)\Delta c_{\mathrm{HbO}}(k) + \alpha_{\mathrm{HbR}}(\lambda_i)\Delta c_{\mathrm{HbR}}(k) + \alpha_{\mathrm{H_2O}}(\lambda_i)\Delta c_{\mathrm{H_2O}}(k), \quad (2)$$

where λ_i is respective wavelength [$i = 1,2,3$] and k is the discrete time. Now the absorbance at required wavelengths can be found by using the value measured by (2). As we are going to find the concentration change of only HbO and HbR so we can find them by using parameters of only two wavelengths:

$$\Delta A_1^*(k, \lambda) = d^{\lambda_1} l\left(\Delta\mu_a^{\lambda_1} - \alpha_{\mathrm{H_2O}}^{\lambda_1}\Delta c_{\mathrm{H_2O}}(k)\right),$$
$$\Delta A_3^*(k, \lambda) = d^{\lambda_3} l\left(\Delta\mu_a^{\lambda_3} - \alpha_{\mathrm{H_2O}}^{\lambda_3}\Delta c_{\mathrm{H_2O}}(k)\right). \quad (3)$$

Now we calculate the concentration change for HbO and HbR again using the absorbance change calculated after subtracting the water factor for wavelength λ1 and λ3. λ1 and λ3 are chosen because they give the best results

$$\begin{bmatrix} \Delta c_{\mathrm{HbO}}(k) \\ \Delta c_{\mathrm{HbR}}(k) \end{bmatrix} = \begin{bmatrix} d^{\lambda_1} l \alpha_{\mathrm{HbO}}^{\lambda_1} & d^{\lambda_1} l \alpha_{\mathrm{HbR}}^{\lambda_1} \\ d^{\lambda_3} l \alpha_{\mathrm{HbO}}^{\lambda_3} & d^{\lambda_3} l \alpha_{\mathrm{HbR}}^{\lambda_3} \end{bmatrix}^{-1} \times \begin{bmatrix} \Delta A_1^*(k, \lambda) \\ \Delta A_3^*(k, \lambda) \end{bmatrix}. \quad (4)$$

To demonstrate the feasibility of accessing the hemodynamic cortical signals, the subjects were directed to perform two-digit arithmetic tasks randomly appearing on a computer screen. Each experiment consisted of six sessions and each session is composed of a 24-s rest and a 15-s task period. Optical probe was positioned in horizontal direction just over the subject's eyebrows.

Fig. 2 shows the experimental paradigm and the results by calculating mean from all sessions of one experiment from Ch 8 of Subject 2 (due to the high concentration level of H_2O) during the experiment. As is consistent with previous literature,[2,19] during the first 24 s of rest period, there was not much change in the concentrations, whereas during the next 15 s of activity period, the HbO and H_2O concentrations increases and the HbR concentration decreases. After the activity period the concentrations come to normal positions.

The water-absorption correction algorithm was used to improve the HbO and HbR signal strengths. Fig. 3 shows that after application of the algorithm, the changes in HbO and HbR concentrations at the least active channel during the activity period, theretofore not clearly visible, were obvious. As the graph indicates, after application of the water-absorption correction algorithm, the magnitude of the corrected HbO signal representing the activity period (the black solid line) increased very significantly compared with that of the uncorrected HbO signal (the red dotted line). Correspondingly, the magnitude of the HbR signal corrected by water-absorption

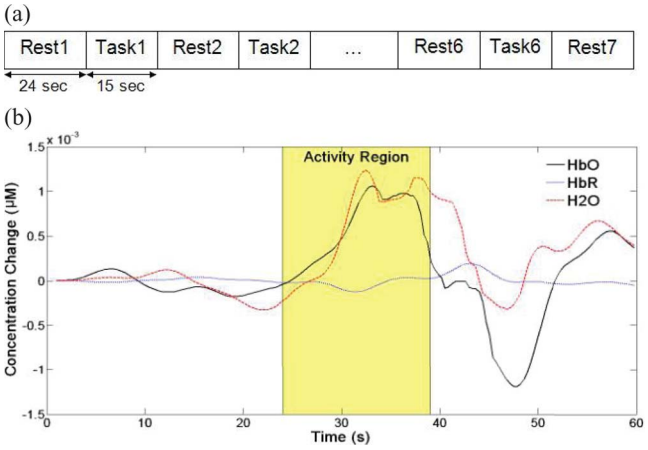

FIG. 2. Arithmetic task experiment: (a) experimental paradigm, (b) concentration changes of HbO, HbR, and H_2O in Ch 8 of Subject 2.

(the blue dashed line) decreased sharply relative to the uncorrected HbR signal (the blue dotted line). Table I gives the percentage increase and decrease in HbO and HbR signals, respectively, after applying the water-absorption correction algorithm. The data for this table are taken as the mean of all the channels for each subject. It is clear from the table that there is a significant change in HbO and HbR signal strength after applying the water-absorption correction algorithm in each subject. The average signal amplitude increased by 271% for HbO and decreased by 261% for HbR. While applying the proposed algorithm, the concentration of H_2O has been subtracted so we are left only with the concentrations of HbO and HbR. Now when we apply the MBLL again it was expected that, concentration change of HbO should increase and HbR should decrease as per the previous literature[15] because the effect due to water has been eliminated so the remaining chromophores will act more prominently as compared to the previous calculations. The results presented in Fig. 3 and Table I are in accordance with the expectations and prove the efficiency of water-absorption correction algorithm proposed in this study.

The present study demonstrated the validity, functionality and effectiveness of a new multichannel NIRS system

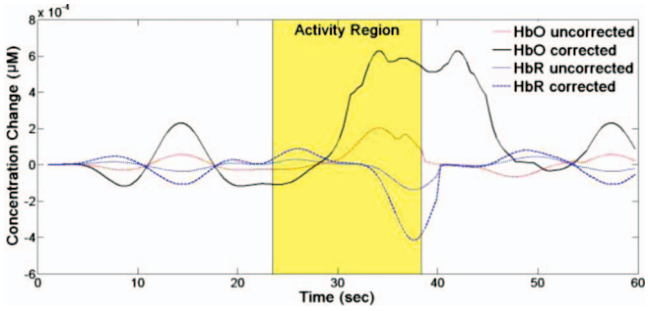

FIG. 3. Comparison of concentration changes of HbO and HbR before and after water-absorption correction: To illustrate the amplification effect of water-absorption compensation, the data of Ch 9 from Subject 5 have been shown since it is the least active channel.

TABLE I. Percentage increase and decrease in HbO/HbR signals for all five subjects.

Subject no.	Mean HbO/HbR uncorrected $\times 10^{-5}$	Mean HbO/HbR corrected $\times 10^{-4}$	% increase and decrease in HbO / HbR %
1	6.780/−0.7758	2.213/−0.2764	226/255
2	7.018/−0.7163	2.611/−0.2467	271/243
3	6.442/−0.6924	2.675/−0.2115	236/205
4	6.231/−0.6548	2.409/−0.2586	227/294
5	6.624/−0.6819	2.751/−0.2810	310/312
Average	6.619/−0.7043	2.453/−0.2543	271/261

employing three tri-wavelength light emitters to determine mental-activity-effected concentration changes in the HbO, HbR, and H_2O. Application of the system's water-absorption correction algorithm enabled the HbO and HbR signals to be shown more actively during the task session. Moreover, the device, thanks to its wireless transmission utility, can easily be used in indoor, outdoor, and/or remote applications.

This work was supported by the National Research Foundation of Korea funded by the Ministry of Education, Science and Technology, Korea (Grant No. MEST-2012-R1A2A2A01046411)

[1]F. F. Jobsis, Science **198**, 1264 (1977).
[2]F. Scholkmann, S. Kleiser, A. Metz, R. Zimmermann, J. M. Pavia, U. Wolf, and M. Wolf, NeuroImage **85**, 6 (2014).
[3]A. Torricelli, D. Contini, A. Pifferi, M. Caffini, R. Re, L. Zucchelli, and L. Spinelli, NeuroImage **85**, 28 (2014).
[4]Y. Lin, G. Lech, S. Nioka, X. Intes, and B. Chance, Rev. Sci. Instrum. **73**, 3065 (2002).
[5]C.-K. Kim, S. Lee, D. Koh, and B.-M. Kim, Biomed. Eng. Lett. **1**, 254 (2011).
[6]J. Bhattacharyya, M. Wagner, S. Zybell, S. Winnerl, D. Stehr, M. Helm, and H. Schneider, Rev. Sci. Instrum. **82**, 103107 (2011).
[7]X.-S. Hu, K.-S. Hong, and S. S. Ge, Neurosci. Lett. **504**, 115 (2011).
[8]M. Kiguchi, H. Atsumori, I. Fukasaku, Y. Kumagai, T. Funane, A. Maki, Y. Kasai, and A. Ninomiya, Rev. Sci. Instrum. **83**, 056101 (2012).
[9]Z. Zhang, B. Sun, H. Gong, L. Zhang, J. Sun, B. Wang, and Q. Luo, Rev. Sci. Instrum. **83**, 094301 (2012).
[10]X.-S. Hu, K.-S. Hong, and S. S. Ge, J. Neural. Eng. **9**, 026012 (2012).
[11]N. G. Lee, S. K. Kang, D. R. Lee, H. J. Hwang, J. H. Jung, J. H. You, C. H. Im, D. A. Kim, J. A. Lee, and K. S. Kim, Arch. Phys. Med. Rehabil. **93**, 882 (2012).
[12]N. Naseer and K.-S. Hong, Neurosci. Lett. **553**, 84 (2013).
[13]Y. Zheng, Z. Zhang, Q. Liu, C. Cao, and H. Gong, Proc. SPIE **6047**, 60470X (2006).
[14]L. Pollonini, R. Re, R. J. Simpson, and C. C. Dacso, Proc. IEEE Eng. Med. Biol Soc. **2012**, 3760.
[15]A. J. Metz, M. Biallas, C. Jenny, T. Muehlemann, and M. Wolf, Adv. Exp. Med. Biol. **765**, 169 (2013).
[16]T. Muehlemann, D. Haensse, and M. Wolf, Opt. Express **16**, 10323 (2008).
[17]L. Kocsis, P. Herman, and A. Eke, Phys. Med. Biol. **51**, N91 (2006).
[18]H. Zhao, Y. Tanikawa, F. Gao, Y. Onodera, A. Sassaroli, K. Tanaka, and Y. Yamada, Phys. Med. Biol. **47**, 2075 (2002).
[19]H. Santosa, M. J. Hong, S.-P. Kim, and K.-S. Hong, Rev. Sci. Instrum. **84**, 073106 (2013).
[20]UCL Department of Medical Physics and Bioengineering, "Specific Extinction Spectra of Tissue Chromophores," See http://www.medphys.ucl.ac.uk/research/borl/research/NIR_topics/spectra/spectra.htm.